2020

The Effect of Cutting Edge Geometry, Nose Radius and Feed on Surface Integrity in Finish Turning of Ti-6Al4V

Ian S. Brown
University of Kentucky, iansbrowninc@gmail.com

Julius M. Schoop
University of Kentucky, julius.schoop@uky.edu

Available online at www.sciencedirect.com

ScienceDirect

Procedia CIRP 87 (2020) 142–147

www.elsevier.com/locate/procedia

5th CIRP CSI 2020

The effect of cutting edge geometry, nose radius and feed on surface integrity in finish turning of Ti-6Al4V

Ian Brown[a,b], Julius Schoop*[a,b]

[a]Department of Mechanical Engineering, University of Kentucky, Lexington, KY, 40506, USA
[b]Institute for Sustainable Manufacturing, University of Kentucky, Lexington, KY, 40506, USA

* Corresponding author. Tel.: 859-323-8308. *E-mail address:* julius.schoop@uky.edu

Abstract

While the respective effects of nose radius, feed and cutting edge geometry on surface integrity have each been studied at depth, coupling between these effects is not yet sufficiently understood. Recent studies have clearly established that cutting edge micro-geometries may not only have positive effects on tool-life, but can also be used to tailor surface integrity characteristics, such as surface roughness and near-surface severe plastic deformation. To further a more fundamental understanding of the effects of cutting edge micro-geometries on surface integrity, experimental turning data was generated for a varied range of cutting tool geometries and feeds. Scanning laser interferometry was used in conjunction with a recently developed profile-analysis algorithm to analyze, characterize, and verify the geometry of complex cutting edge micro-geometries. Near surface nanostructure, and surface roughness of the produced surfaces were characterized and correlated to the varied tool geometries. An interaction between two geometry characteristics, predicted kinematic roughness and hone size, was discovered. Scanning laser interferometry analysis of the surfaces revealed that large hones provided either an increase or decrease in roughness, depending on predicted kinematic roughness.

Keywords: Surface integrity, Roughness, Finishing, Kinematics, Machining

1. Introduction

The influence of tool geometry on machining processes is highly significant and can be approached from many different angles. Not only do optimal tool geometries provide opportunities for increased process efficiency in the form of tool-life [1], these same geometric tool parameters also have significant impacts on component surface integrity. Depending on a tool's micro-geometry (e.g., cutting edge radius) and macro-geometry (e.g., nose radius), surface integrity properties like surface roughness and microstructural changes may be varied significantly [2]. Moreover, these effects are exaggerated in finish machining as the uncut chip thickness size begins to approach the size of the hone of the cutting tool, making the resulting properties of the machined surface highly dependent on the condition and quality of the selected tool [3]. Therefore, a firm understanding of the influence of tool geometry on surface integrity of machined parts is necessary for optimum machining performance.

The effects of cutting edge micro-geometry on the machining process as a whole have since been studied to great extent, as outlined by Denkena in [4]. Specifically, the influence of cutting edge micro-geometry on surface integrity has been investigated at depth. One of the most prominent effects produced by different tool micro-geometries is the ploughing effect. Albrecht introduced the idea of ploughing due to edge rounding in metal-cutting tools in 1960 [5]; ploughing has been described as the

10.1016/j.procir.2020.02.039

plastic displacement of material to the side or ahead of the cutting direction, rather than the forming of a chip [6].

Thiele et al. [3] describe the effects of radial hone and chamfered edge geometries on the surface roughness in bearing steel, citing ploughing as a major contributor to roughness and observed forces in finish-machined surfaces. Segebade et al. investigated waterfall-honed (or ellipsoidal/asymmetrical) cutting geometries and found a correlation with the depth of the grain-refined surface layer [7]. Generally, larger cutting edge geometry features have been found to create deeper grain-refined layers [8].

Another commonly varied tool geometry parameter that has influence over surface integrity is nose radius. The effect of nose radius on surface roughness is easy to visualize due to the obvious geometric link between kinematic (i.e., theoretical geometric) roughness, nose radius and feed. At a given feed rate, decreasing the nose radius will increase roughness; however, at very low feeds, such as those found in finish machining, large nose radii begin to plough much more than smaller nose radii, leading to higher roughness than predicted by the kinematic roughness equation (see Eq. 1). This effect has long been qualitatively understood to be due to chip thinning [9]. Sharman et al. [10] has shown that increasing tool nose radius increased ploughing forces and microstructural deformation depth in Inconel 718. Chou et al. [9] found that the depth of the heat-affected microstructural layer varied depending on both the condition of the tool and the nose radius in AISI 52100 steel.

Therefore, both cutting edge radius and nose radius are then understood to affect the surface integrity of machined surfaces; however, there exists little experimental knowledge of the interactions that exist between the two parameters in the realm of surface integrity. The presented work is pointed to discuss this area in order to further a more complete understanding of the surface integrity induced by finishing processes.

Nomenclature

CNC	Computer Numerical Control
FIB	Focused Ion Beam
ICEME	Integrated Computational and Experimental Manufacturing Engineering Laboratory
MPM	Surface Meters per Minute
SEM	Scanning Electron Microscope
SPD	Severe Plastic Deformation

2. Experimental Setup

In order to observe the behavior of interactions between the nose radius and cutting edge micro-geometry, dry finish face turning was performed on a 3-inch diameter bar of Ti-6Al4V workpiece material. The machine tool used to perform these tests was a HAAS TL-2 CNC lathe and the cutting tools used were modified Kennametal TPGN (triangle) geometries of the uncoated, fine-grained carbide grade K68. The conditions that were varied for each test included feed, edge micro-geometry, and nose radius, as outlined in Table 1. All other variable parameters were held constant. Constant parameters of some consequence include cutting speed (v_c), held at 288 MPM, depth of cut (a_p), held at 0.25mm. Note that the 40:20µm edge value represents a non-uniform edge hone that is biased toward the flank face of the cutting tool. This characterization methodology is known as the K-factor method, detailed by Denkena et al. in [11]. In this study, tools that have a K-factor of K=1 are conventional, uniform hone tools with constant radius.

Table 1. Overview of full-factorial DOE variables. Reference

Factors:	Cutting Edge	Nose Radius	Feed
	5µm; K=1	0.4mm	0.1mm
	35µm; K=1	0.8mm	0.2mm
	50µm; K=1	1.6mm	
	40:20µm; K=2	3.2mm	

After each face turning test condition, the machined surface was parted off the main bar at 6mm thickness for subsequent analysis. Prior to each test condition, the workpiece face was chamfered and cleaned up with an unworn sharp tool to standardize initial conditions. In total, 32 test specimens were collected. Each of these test specimens had unique conditions, therefore each condition was performed once. Cutting forces were ascertained by a KISTLER type 9257B three-channel dynamometer. Thermal imaging was acquired by a FLIR SC7000 series camera in conjunction with ResearchIR analysis software. The dynamometer and thermal imaging apparatus are shown in Fig. 1 below.

Fig. 1. Experimental turning setup used to obtain data discussed herein.

Post-experiment analysis was conducted with instrumentation including a Zygo NewView 7300 scanning laser interferometer, which was used to create pointcloud maps, from which roughness data were drawn using Zygo MX software. Imaging of the surface nanostructure was achieved via Thermo Scientific Helios NanoLab DualBeam SEM/FIB microscope. Specifically, the nanostructure was exposed by FIB milling the machined surface in order to create deformation-free cross-sections. Images of these cross-sections were then obtained by deploying low-amperage FIB imaging, which showed high contrast between the individual grains and phases of the sample material. No destructive sample preparation was utilized before insertion of the sample into the microscope due to this method.

The preparation of experimental cutting tool edges was accomplished by a novel honing method developed by the authors that creates hones with final geometry accuracy variance of less than 20%. This method relies upon the use of a HAAS VF-2 CNC milling machine equipped with a diamond-paste impregnated buffing wheel. An example of a honed cutting edge profile, as well as the basic methodology used to characterize them, is shown below.

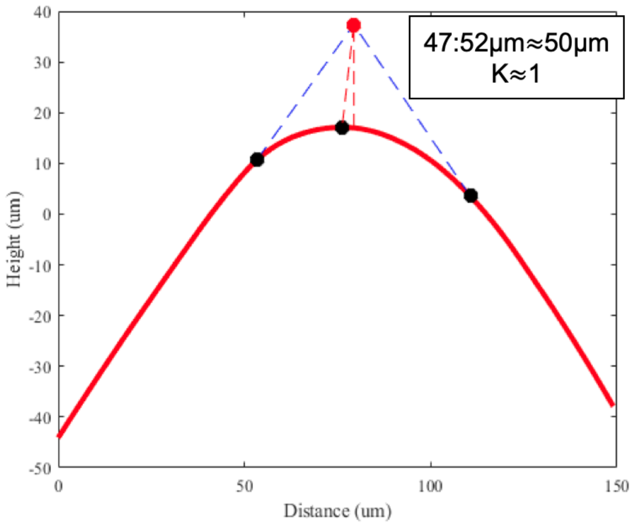

Fig. 2. Example of characterization method employed to analyze the cutting edge micro-geometry of cutting tools used in the experiment.

Validation of the individual cutting edge geometries of each tool was achieved by the use of an automated MATLAB code (developed in the authors' lab at the University of Kentucky) which interprets Zygo-created pointcloud maps of the cutting edge to assign edge radii and K factor values (soon to be released on GitHub). Additionally, a custom fixture was utilized to locate each edge in a reliable, unbiased manner before creating each pointcloud map.

3. Results and Discussion

3.1. Surface Roughness: Influence of Size Effects

A key finding discovered through detailed analysis of the surfaces generated by these experiments was that nose radius, feed and the size of the cutting-edge hone were found to have an interaction effect on the observed roughness of the samples. When considering that both radius and feed affect the topology of the machined surface in a similar, geometric way, it is evident that variances in either of them would have similar effects upon the produced surface roughness. Due to this observation, much of the subsequent analysis treats nose radius and feed as a single factor that is more relative to this study: predicted kinematic roughness. The equation used to arrive at this new value for a given nose radius and feed is shown below in Equation (1).

$$Kinematic\ Roughness = \frac{f^2}{32*r} \qquad (1)$$

Where f is the feed and r is the tool nose radius. Additionally, to better understand the phenomena described in this study, it is helpful to illustrate the role of predicted kinematic roughness and minimum chip thickness on the behavior of ploughing, including how these values are affected by cutting edge geometry and nose radius.

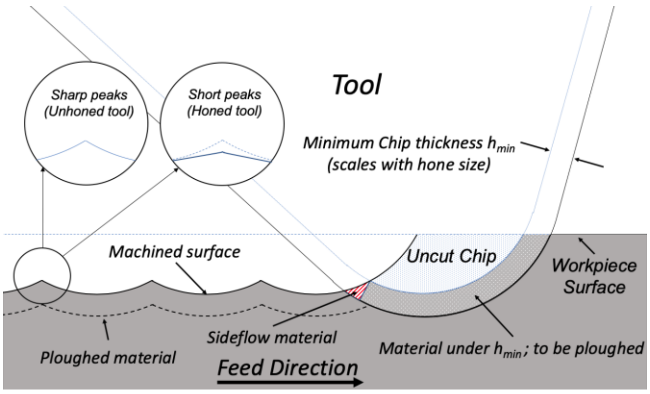

Fig. 3. Geometrical model of a turning process clarifying the influence of ploughing effects on roughness at higher kinematic roughness values. Note that h_{min} is meant to denote minimum chip thickness.

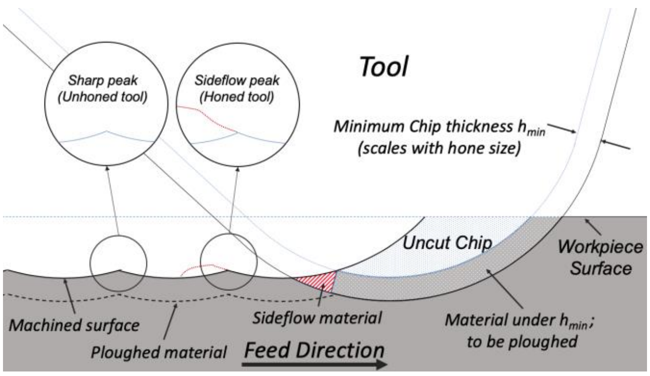

Fig. 4. Geometrical model of a turning process depicting ploughing effects on roughness at lower kinematic roughness values. Note that h_{min} is meant to denote minimum chip thickness.

Chip thinning is a well-known consequence of reducing feed or increasing tool nose radius. The second model above shows a thinner chip relative to the first model due to an increase in nose radius. This effect leads to an elongation of the chip in addition to the thinning effect. Machining with lower chip thickness generally leads to better surfaces. However, at very thin chip thicknesses, ploughing begins to dominate and influences machined surfaces negatively. This is understood to be due in large part to displacement of material around the tool, rather than into the chip. Large cutting edge radii can cause an increase in minimum chip thickness (defined as the minimum depth of cut that will allow for a chip to be removed from the material), which will allow more material to be displaced under and around the tool as it progresses along the part surface. Increases in both of these parameters will cause a higher volume of material to be ploughed into the machined surface, relative to the material removed. Both of these parameters influence the size of the theoretical uncut chip zone that is prone to sideflow, as shown in Fig. 3 and Fig. 4.

Upon observation of the machined surfaces, an increase in hone size was found to increase observed surface roughness for conditions with very low predicted kinematic roughness levels. This effect can be seen in Fig. 5, specifically the portion of the data found to the left of the inflection point. This has been documented thoroughly and, as discussed previously, is understood to be an effect of the additional ploughing material introduced into the workpiece surface, i.e. a so-called 'size effect' [4, 12-14]. However, this study presents another finding in addition to this: complex interactions between predicted kinematic roughness and cutting edge radius on surface roughness. As predicted kinematic roughness for the various conditions increased to ~0.4μm Ra, the actual roughness values showed an inversion of the trend established at lower roughness levels. This inversion of the hone and kinematic roughness relationship is clearly displayed in Fig. 5. As previously established, roughness values still increased with hone at very fine predicted kinematic roughness; however, above predicted kinematic roughness of ~0.4μm Ra, roughness tended to decrease with increases in hone size.

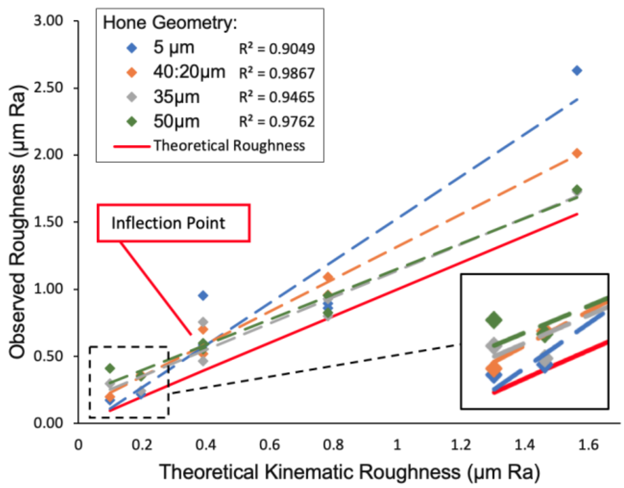

Fig. 5. Graph showing the roughness trends for each hone.

For predicted kinematic roughness values under ~0.4μm Ra, roughness tended to increase when a relatively large 50μm hone was used, while sharper tools led to significantly smoother surfaces. This effect is the result of the coupling of two factors that encourage ploughing. These factors are chip thinning, caused by the use of larger nose radii and lower feed, coupled with the increased minimum chip thickness increase, caused by the larger hone. In combination, these factors lead to excessive ploughing of the surface and create a large amount of side flow, which increases the surface roughness of the otherwise theoretically smoother surface that would be generated with these parameters with perfectly sharp tools. This increased material volume that is directed towards the side of the tool, increasing roughness, is represented geometrically in Fig. 3 and Fig. 4 and labeled "sideflow material".

Previous studies have anecdotally noted that process stability is reduced for fine finishing with honed tools, as a ploughing condition generates higher forces than 'cleaner' cutting conditions, leading to vibration and deflection of the machine tool and workpiece. In the present study, this effect was indeed displayed most prominently in tools with larger radius that were used in the fine feed condition. The pointcloud map in Fig. 6b shows severe waviness in the machined part that was found to contribute significantly to the high observed roughness value for that condition.

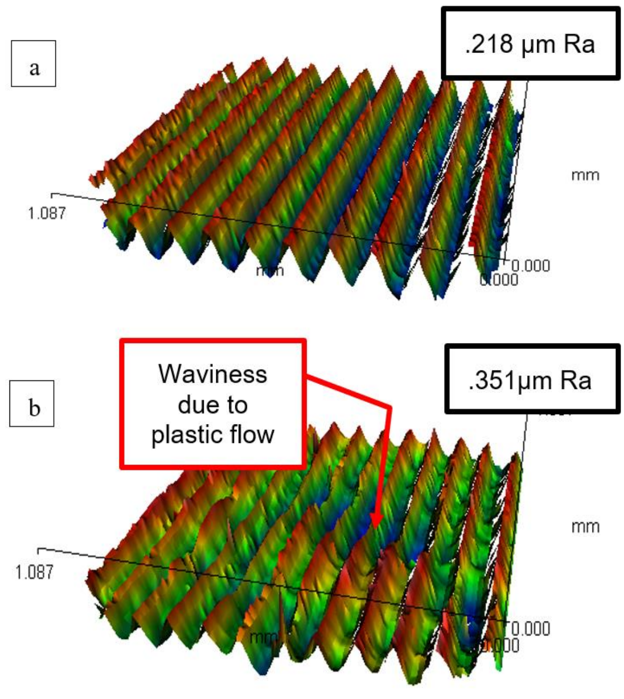

Fig. 6. Laser interferometer-generated surfaces showing the roughness increase due to sideflow and stability issues cutting with larger hones for the same nose radius. a) 1.6mm nose radius, 0.1mm feed, 5μm hone. b) 1.6mm nose radius, 0.1mm feed, 50μm hone.

For predicted kinematic roughness values over ~0.4μm Ra, roughness values were found to increase with a decrease in hone, rather than an increase in hone, as previously shown to the left of the inflection point in Fig. 5. Sharper tools tended to generate higher surface roughness relative to tools with larger hones when predicted kinematic roughness was higher. This inversion phenomenon can be explained relative to the ploughing theory as explained previously. Roughness at these parameters is effectively decreased by ploughing effects of the honed tools. The ploughing-dominated surface generation found at these parameters leads to lower peak height between passes as shown in Fig. 7. The samples with higher peak heights were also noted to have peaks with a slight bias away from the feed direction. This effect is likely caused by the taller peaks' geometry, as a thinner cross section is more likely to deform under load than one that has supporting material around it.

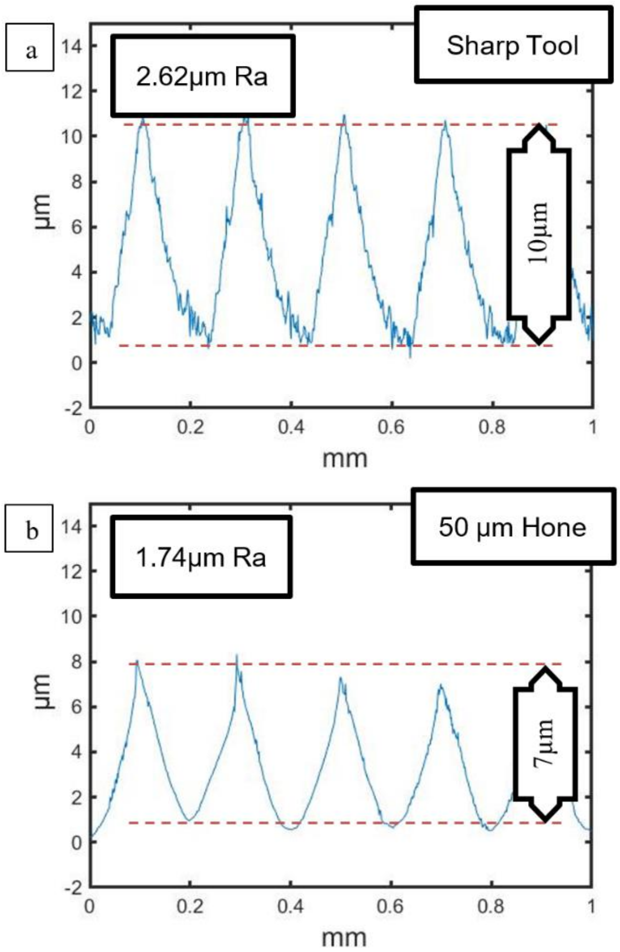

Fig. 7. Laser interferometer-generated surface cross sections showing the relative differences of roughness profiles at higher kinematic roughness. a) 0.8mm nose radius, 0.2mm feed, 5μm hone. b) 0.8mm nose radius, 0.2mm feed, 50μm hone.

These effects are not as relevant at machining parameters with low predicted kinematic roughness, as the geometry of the theoretical roughness is already close to a flat surface. For any ploughing-induced change in peak height, there is less comparative change possible. Surfaces produced at low predicted kinematic roughness are still somewhat subject to these effects, however the effect on roughness is relatively small when compared to the roughness increase caused by the surface-disturbing plastic-flow element of the ploughing action discussed previously.

Moreover, this reduction in surface roughness at higher hones can be further explained by process stability. Previous studies have noted increased process stability due to honed tools; typical cutting action is damped by visco-plastic deformation and thus less prone to vibration when used at appropriate feeds and speeds [15, 16]. The lack of this effect has been shown to increase the effective roughness values dramatically when relatively sharp tools are used. The cutting action of such tools causes much less ploughing, and thus the ploughing-induced dynamic stability is reduced accordingly.

3.2. Near-surface Refined Layers

Nanostructure was preliminarily investigated in 4 representative samples, using an advanced FIB/SEM hybrid characterization technique. Fig. 8 and Fig. 9 illustrate the typical morphology of this layer. The modified microstructural layer can be described as having two distinct layers: a layer of severe plastic deformation (SPD) and recrystallization near the tool/workpiece interface, and a transition layer of less-severely affected material which separates the undeformed bulk from the SPD layer. This layer generally follows a gradient of microstructural change, decreasing in damage level as distance from the machined surface increases. The measurements depicted and used for analysis here are based on the transition layer/ bulk interface.

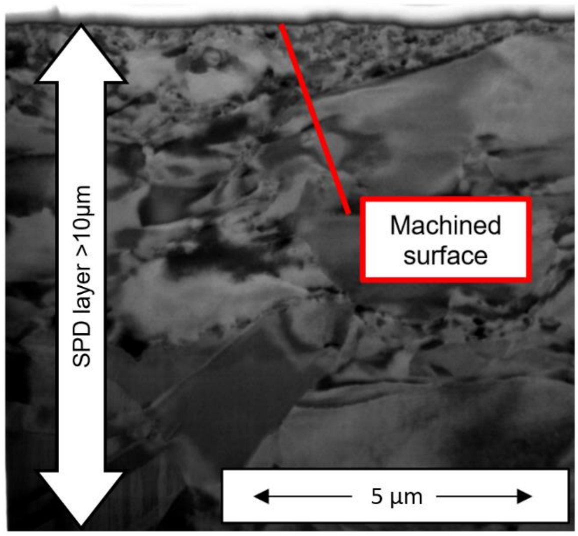

Fig. 8. FIB micrograph of near-surface microstructure of sample machined with 50μm hone, 0.4mm tool nose radius and 0.1mm feed. The SPD layer continues well into the subsurface. FIB microscopy, 10000x.

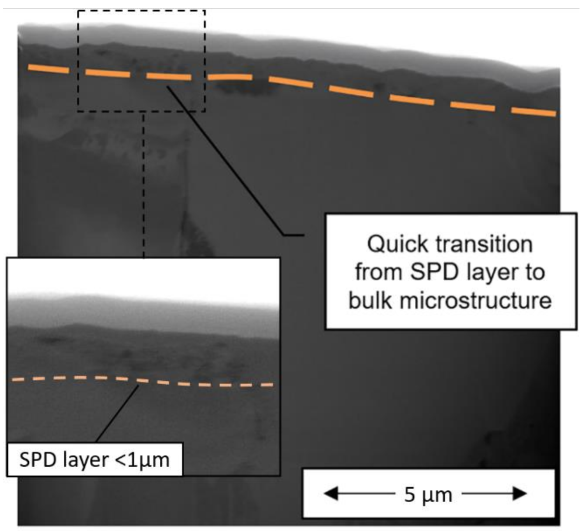

Fig. 9. FIB micrograph of near-surface microstructure of sample machined with 5μm hone edge, 0.4mm tool nose radius and 0.1mm feed. FIB microscopy, 8000x.

As can be seen in the preceding figures, affected microstructural layer generally increases with hone size. These results loosely verify the trends and hypotheses defined in the previous sub-section regarding minimum chip thickness size effects. Under the severely deforming effects of a large 50µm hone, the discussed ploughing behavior is made evident by the observed microstructure. Conversely, the 5µm cutting edge left nearly no evidence of disturbed material. It is hypothesized that upon further inspection of the remaining samples a trend between the affected microstructure layer depth and the nose radius may be identified.

4. Conclusions

This paper primarily seeks to compare and deconvolute surface integrity effects caused by relationships between different turning geometrical parameters. To this end, the following conclusions can be summarized based on experimental data and preliminary modeling efforts:

- For higher values of predicted kinematic roughness, cutting edge geometries with larger hones were found to reduce the roughness of the machined surface, while conditions with lower values of predicted kinematic roughness caused the larger hones to produce surfaces with increased roughness due to ploughing effects.

- Side flow and instability effects increase roughness and dominate conditions at low kinematic roughness parameters, while the reduction of peak height and greater process stability is responsible for reducing roughness at higher kinematic roughness conditions.

- Additional data in the form of microstructural damage layer depth corroborate the main argument and verify existing assumptions about ploughing and surface roughness.

- Future work will be pointed at the modeling of other surface integrity values, as well as investigation into the effect of the relative depth of microstructural damage relative to the interaction between predicted kinematic roughness and cutting edge radius.

Acknowledgements

The authors would like to gratefully acknowledge support by the University of Kentucky’s Department of Mechanical Engineering, Institute for Sustainable Manufacturing and Electron Microscopy Center.

References

[1] Casto SL, Passannanti G, and Ippolito R. On the influence of the radius between face and flank on the tool life of sintered carbides. CIRP Annals, 1985. 34(1): p. 83-85.
[2] Bedekar V, et al. Nanostructural evolution of hard turning layers in response to insert geometry, cutting parameters and material microstructure. CIRP Annals, 2013. 62(1): p. 63-66.
[3] Thiele JD and N. Melkote S. Effect of cutting edge geometry and workpiece hardness on surface generation in the finish hard turning of AISI 52100 steel. Journal of Materials Processing Tech, 1999. 94(2): p. 216-226.
[4] Denkena B and Biermann D. Cutting edge geometries. CIRP Annals - Manufacturing Technology, 2014. 63(2): p. 631-653.
[5] Albrecht P. New Developments in the Theory of the Metal-Cutting Process: Part I. The Ploughing Process in Metal Cutting. Journal of Engineering for Industry, 1960. 82(4): p. 348-357.
[6] Samuels LE. Metallographic polishing by mechanical methods. 3rd ed. ed. 1982, Metals Park, Ohio: Metals Park, Ohio : American Society for Metals.
[7] Segebade E, Zanger F, and Schulze V. Influence of Different Asymmetrical Cutting Edge Microgeometries on Surface Integrity. Procedia CIRP, 2016. 45: p. 11-14.
[8] Jivishov V. Mikrogeometrische Einflüsse beim Weich-und Hartspanen. 2008: PZH, Produktionstechn. Zentrum.
[9] Chou YK and Song H. Tool nose radius effects on finish hard turning. Journal of Materials Processing Technology, 2004. 148(2): p. 259-268.
[10] Sharman ARC, Hughes JI, and Ridgway K. The effect of tool nose radius on surface integrity and residual stresses when turning Inconel 718™. Journal of Materials Processing Tech, 2015. 216: p. 123-132.
[11] Denkena B, et al. Surface preparation, coating and wear performance of geometrically defined cutting edges. in Proceedings of the 5th international conference the coatings in manufacturing engineering. 2005.
[12] Özel T. Computational modelling of 3D turning: Influence of edge micro-geometry on forces, stresses, friction and tool wear in PcBN tooling. Journal of Materials Processing Technology, 2009. 209(11): p. 5167-5177.
[13] Özel T, Hsu T-K, and Zeren E. Effects of cutting edge geometry, workpiece hardness, feed rate and cutting speed on surface roughness and forces in finish turning of hardened AISI H13 steel. The International Journal of Advanced Manufacturing Technology, 2005. 25(3): p. 262-269.
[14] Burhanuddin Y, Che Haron CH, and Ghani JA. The Effect of Tool Edge Geometry on Tool Performance and Surface Integrity in Turning Ti-6Al-4V Alloys. 2011. p. 1211-1221.
[15] Denkena B, Koehler J, and Rehe M. Influence of the Honed Cutting Edge on Tool Wear and Surface Integrity in Slot Milling of 42CrMo4 Steel. Procedia CIRP, 2012. 1: p. 190-195.
[16] Biermann D and Baschin A. Influence of cutting edge geometry and cutting edge radius on the stability of micromilling processes. Production Engineering, 2009. 3(4-5): p. 375-380.